Journal of Non-Crystalline Solids 560 (2021) 120754

Contents lists available at ScienceDirect

Journal of Non-Crystalline Solids

journal homepage: www.elsevier.com/locate/jnoncrysol

High-frequency elastic moduli and internal frictions of $Zr_{41.2}Ti_{13.8}Cu_{12.5}Ni_{10}Be_{22.5}$ bulk metallic glass during glass transition and crystallization

Mingyu Xie [a,b,1], Gan Ding [c,d,1], Minqiang Jiang [c,e,*], Faxin Li [a,b,*]

[a] LTCS and College of Engineering, Peking University, Beijing 100871, China
[b] Center for Applied Physics and Technology, Peking University, Beijing, China
[c] State Key Laboratory of Nonlinear Mechanics, Institute of Mechanics, Chinese Academy of Sciences, Beijing 100190, China
[d] State Key Laboratory for Mechanical Behavior of Materials, Xi'an Jiaotong University, Xi'an 710049, China
[e] School of Engineering Science, University of Chinese Academy of Sciences, Beijing 100049, China

ARTICLE INFO

Keywords:
Bulk metallic glass
Elastic moduli
Internal frictions
Glass transition
Crystallization

ABSTRACT

Temperature dependent Young's modulus, shear modulus and the related internal frictions of $Zr_{41.2}Ti_{13.8}Cu_{12.5}Ni_{10}Be_{22.5}$ (Vit-1) bulk metallic glass (BMG) were measured by using the modified piezoelectric ultrasonic composite oscillator technique (M-PUCOT) at longitudinal and torsional resonance under several tens of kilohertz, respectively. An irreversible internal friction peak accompanied by a very small modulus relaxation (about 10%) are observed near the onset crystallization temperatures T_x in each resonance mode, and the peak values in these two modes are almost the same, indicating that the supercooled liquid region (SLR) is far from liquid state under high frequency vibration with micro strain ($\sim 10^{-7}$) amplitude. What is more, the internal friction peak value decreases obviously after a preheating process to SLR (~410 °C) and the final values of moduli are proportional to the crystallinity. All these interesting phenomena during the glass transition and crystallization can well be interpreted through a three-parameter anelastic solid phenomenological model.

1. Introduction

Bulk metallic glass (BMG) possesses superhigh strength, good glass forming capacity and wide supercooled liquid region (SLR), which has potentials for various applications and provides great convenience for various researches [1–3]. In recent years, of great interest are the mechanism of glass transition and crystallization of the BMG. Intensive investigations has been carried out on the measurement of the changes of the viscosity [4], electrical resistivity [5], and thermal expansion [6] of the BMG during glass transition and crystallization. In fact, the elastic moduli and related internal frictions are very sensitive to the microstructural of the BMG and can be used as probes revealing the process of structural transformation.

Previous experimental studies on elastic moduli and internal frictions of the BMG were either using a torsion pendulum [7–9] or commercial dynamic mechanical analyzer (DMA) [10,11] at very low frequency (~1 Hz), and the simultaneous study of Young's modulus, shear modulus and their related internal frictions were seldom reported. For the inverted torsion pendulum, the measured frequency and internal friction depend on the properties of both the specimen and the suspension wire, and if there is no calibration, there will be large deviations between the measured internal friction and the actual internal friction [9]. Commercial DMA is usually limited to the measurement of polymers, plastics or other soft materials, and the measurement accuracy on metals is quite low. Ichitsubo [12,13] investigated the elastic and anelastic properties of the BMG near the onset glass transition temperature T_g using the electromagnetic acoustic resonance (EMAR) technique at ultrahigh frequency (~500 kHz). However, complicated modal identification is required for EMAR, and the elastic moduli and internal frictions cannot be measured simultaneously. It has been shown that time is a critical parameter for characterizing the metastable nature of metallic glasses [14], so it is particularly important to monitor the elastic moduli and internal frictions simultaneously.

In the theoretical investigations, the formation of internal friction

* Corresponding authors.
E-mail addresses: mqjiang@imech.ac.cn (M. Jiang), lifaxin@pku.edu.cn (F. Li).
[1] Mingyu Xie and Gan Ding contributed equally.

https://doi.org/10.1016/j.jnoncrysol.2021.120754
Received 2 December 2020; Received in revised form 7 February 2021; Accepted 16 February 2021
Available online 23 February 2021

peak of BMG is still controversial. Li et al. [15] found a reversible internal friction peak near the onset glass transition temperature T_g of $Pb_{77.5}Cu_6Si_{16.5}$. They believed that the original of this peak is completely related to the glass transition without the intervention of crystallization, and proposed a cluster model to explain this phenomenon. Ichitsubo reported an irreversible internal friction peak at T_g of $Zr_{55}Al_{10}Ni_5Cu_{30}$ and attributed them to the atomic motion in the initial glass state [12]. By measuring the low frequency internal friction of different Ni- and Pd-based metal glasses using a Collette torsion pendulum, Sinning point out that the observed peak can be simply attributed to the sharp monotonic increase of the internal friction in the SLR above T_g and the rapid decrease caused by subsequent crystallization [9]. Sinning also used the simple Maxwell model to interpret it. It is worth noting that the above-mentioned theories or models can only be used to interpret the measurement results at very low frequency (~1 Hz) or at ultrahigh frequency (>500 kHz) and an effective model is still lack to explain the mechanical behavior of BMG under several to tens of kilohertz.

In this work, the temperature dependent Young's modulus, shear modulus and two related internal frictions of the $Zr_{41.2}Ti_{13.8}Cu_{12.5}Ni_{10}Be_{22.5}$ bulk metal glass were investigated under tens of kilohertz using a new method called M-PUCOT (modified piezoelectric ultrasonic composite oscillator technique) [16]. First, the measurement principle of M-PUCOT is introduced. Then the measurement results of the BMG are discussed and compared with the DCS and XRD measurement results. Finally, a three-parameter anelastic model was used to interpret these observed phenomena of BMG.

2. Experimental procedure

For the preparation of the specimen, ingots of master alloys were obtained by arc-melting a mixture of pure metals (Zr, Ti, Cu, Ni, Be, purity >99.9 wt.%) in a Ti-gettered high-purity argon atmosphere, and remelted at least 5 times to ensure chemical homogeneity. Then BMG rods with the diameter of 8 mm were prepared by suction casting from master alloys ingots to a water-cooled copper mold in an arc furnace. Specimens with 45 mm long were cut from the as-cast rods, of which both ends were polished carefully to ensure the parallelism. As shown in Fig. 1, in M-PUCOT, we employed a small PZT ring transducer (with outer diameter $D = 8$ mm, inner diameter $d = 4$ mm, thickness $h = 2$ mm) to both drive and gage the vibration. For Young's modulus and longitudinal internal friction measurement, a thickness-poled d_{33}-mode PZT ring with electrodes sprayed on the upper and lower surfaces was used. When an alternating electric field is applied along the thickness direction of the transducers, the longitudinal vibration can be generated. For shear modulus and torsional internal friction measurement, the d_{15}-mode transducer with two lateral electrodes was assembled by two thickness-poled half-rings with the poling direction reversed. A Perfect torsional vibration can be generated when a circumferential alternating electric field is applied. More details of the two transducers are shown in the supplementary materials. A 125.5 mm long alumina spacer with the same diameter was bonded between the specimen and transducer, forming a three-component system to keep the PZT transducer working at an acceptable temperature (The reason for choosing alumina spacer rather than fused quartz spacer is that the mechanical strength of alumina spacer is much higher thus it is more suitable for measuring the materials with large thermal expansion coefficients). The number of half wavelengths in the spacer and specimen was both one. The joint between the spacer and the specimen was arranged near the resonance antinode of the system to eliminate the influence of the high temperature ceramic adhesive on the internal friction measurement. The specimen was inserted in a furnace with the temperature variation less than 1 °C. A thermocouple was placed near the specimen to control and detect the temperature. The influence of temperature gradient in the intermediate alumina spacer can be calibrated and the details are shown in the supplementary material. (Note that even if the calibration was omitted, it has little influence on the calculated moduli and internal frictions of the BMG). By measuring the resonance and anti-resonance frequency of the system's susceptance curve at varied temperature using an impedance analyzer, the temperature dependent Young's modulus (E_M), shear modulus (G_M), longitudinal internal friction (Q_{ML}^{-1}), and torsional internal friction (Q_{MT}^{-1}) of the specimen can be obtained using the following formula [16]:

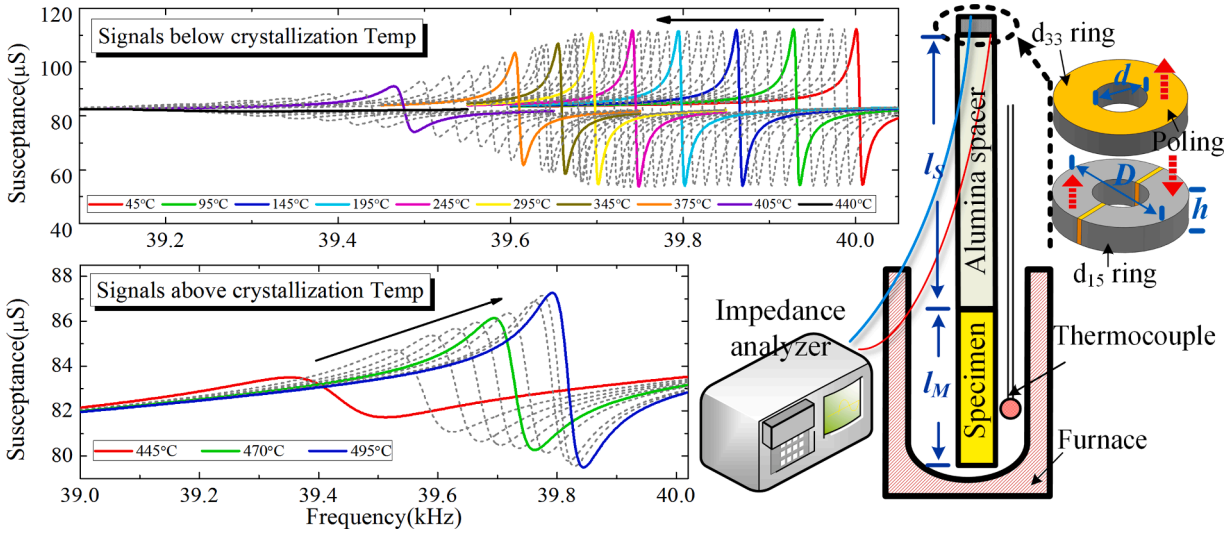

Fig. 1. The experimental setup of M-PUCOT and the measured susceptance curves of the transducer-spacer-specimen (BMG) three-component system for longitudinal vibration during one heating process.

$$\begin{cases} E_M = \left\{ \left[1 + \left(1 - \frac{d^2}{D^2} \right) \frac{\rho_P h}{\rho_M l_M} + \frac{\rho_S l_S}{\rho_M l_M} \right] \frac{f_{m+n}^{rL} + f_{m+n}^{aL}}{2} 2 l_M - \frac{m\sqrt{E_S \rho_S}}{\rho_M} \right\}^2 \frac{\rho_M}{n^2} \\ G_M = \left\{ \left[1 + \left(1 - \frac{d^4}{D^4} \right) \frac{\rho_P h}{\rho_M l_M} + \frac{\rho_S l_S}{\rho_M l_M} \right] \frac{f_{m+n}^{rT} + f_{m+n}^{aT}}{2} 2 l_M - \frac{m\sqrt{G_S \rho_S}}{\rho_M} \right\}^2 \frac{\rho_M}{n^2} \\ Q_{ML}^{-1} = 2 \frac{f_{m+n}^{aL} - f_{m+n}^{rL}}{f_{m+n}^{aL} + f_{m+n}^{rL}} \left(1 + \frac{m\sqrt{E_S \rho_S}}{n\sqrt{E_M \rho_M}} \right) - \frac{m\sqrt{E_S \rho_S}}{n\sqrt{E_M \rho_M}} Q_{SL}^{-1} \\ Q_{MT}^{-1} = 2 \frac{f_{m+n}^{aT} - f_{m+n}^{rT}}{f_{m+n}^{aT} + f_{m+n}^{rT}} \left(1 + \frac{m\sqrt{G_S \rho_S}}{n\sqrt{G_M \rho_M}} \right) - \frac{m\sqrt{G_S \rho_S}}{n\sqrt{G_M \rho_M}} Q_{ST}^{-1} \end{cases} \tag{1}$$

Where l_S and l_M are the length of the spacer and specimen. ρ_P, ρ_S and ρ_M are the density of the transducer, spacer and specimen. E_S, G_S are Young's modulus and shear modulus of the alumina spacer. Q_{SL}^{-1} and Q_{ST}^{-1} are longitudinal and torsional internal friction of the alumina spacer. f_{m+n}^{rL} (f_{m+n}^{rT}) and f_{m+n}^{aL} (f_{m+n}^{aT}) are $(m + n)$-order resonance frequency and anti-resonance frequency of the susceptance curve for longitudinal (torsional) vibration. m and n are the numbers of half-wavelength in the spacer and specimen, and here $m = n = 1$. The voltage applied on the transducer is 1 V, so the strain amplitude during testing is about 10^{-7}. Based on the calibration results of the alumina spacer (see in the supplementary material), the uncertainty of the measured Young's modulus and shear modulus of the BMG are estimated to be 0.2Gpa and 0.1Gpa, respectively. For the two related internal frictions, the uncertainties are about 0.4E-4. Fig. 1 also shows the measured susceptance curves of the transducer-spacer-BMG specimen system for longitudinal vibration during one heating process. It can be seen that, the peak frequencies of the susceptance curves (represent the elastic modulus of the specimen) decrease slowly below the crystallization temperature (T_x=439 °C) but increase rapidly above T_x; The frequency difference between the resonance frequency and the anti-resonance frequency (represent the internal friction of the specimen) almost unchanged below 300 °C, then changed rapidly near the T_x, forming an internal friction peak. Compared with the EMAR technique [12] in which the modal identification is complicated due to the overlapping of the measured signals, the resonance signals measured by M-PUCOT are noiseless and have significant changes during structural transformation. In addition, DSC measurement was conducted using a slice shaped Vit-1 BMG specimen with the same heating rate of 3 °C/min.

3. Results and discussion

Fig. 2 shows the DSC measurement of Vit-1 BMG. Above 375 °C in the DSC curve, we can see a little endothermic step, which represents the glass transition process of the BMG. The start of this step (375 °C) is defined as the onset glass transition temperature T_g. The biggest exothermic peak in DSC curve represents the crystallization process of the BMG, and the beginning of this peak (439 °C) is defined as the onset crystallization temperature T_x. Fig. 3 shows the temperature dependent Young's modulus, shear modulus, longitudinal and torsional internal frictions of the Vit-1 BMG during the heating and cooling processes. It can be seen that, in the initial stage of the heating process, both moduli decrease almost linearly with the increasing temperature, while the internal frictions keep almost unchanged. The initial torsional internal friction ($\sim 1.3 \times 10^{-3}$) is much larger than the longitudinal one (0.48×10^{-3}). When the temperature reaches the T_g of 375 °C, the BMG enters the supercooled liquid region (SLR) and the structure relaxed, resulting in the decrease of moduli and the rapid increase of internal frictions. With the further increase of the temperature, the BMG turns to a deep supercooled state until it begins to crystallize at about 440 °C when both elastic moduli reach the minima, which are about 90% of their initial values. At the same time, an obvious internal friction peak appears in each vibration mode with the peak values both around 16–18 $\times 10^{-3}$. Note that both internal friction peak values are much smaller than that measured by using the low-frequency DMA, which can be even larger than 0.25 [10,17]. When further increasing the temperature, both the Young's modulus and shear modulus increase steadily and both internal frictions drops quickly, indicating that crystallization dominates this stage. Obviously, the crystallization process does not saturate at 500 °C. During the cooling process, the specimen exhibits the characteristics of crystalline metals, i.e., the elastic moduli increase and the internal frictions decrease steadily with the decreasing temperature, and no peak appears.

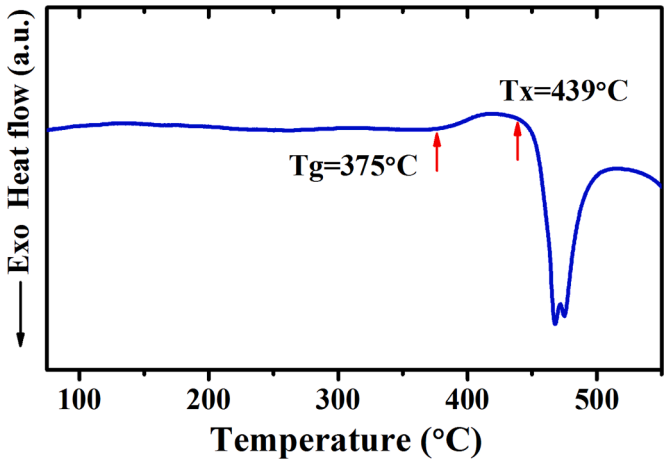

Fig. 2. DSC measurement of Vit-1 BMG.

Partially consistent with Sinning's view [9,18], we agree that the observed internal friction peak can be simply attributed to the sharp monotonic increase of the internal friction in the SLR above T_g and the rapid decrease caused by subsequent crystallization. But at high frequency, we do not accept the point that the glass transition is a transition from a 'solid' state to a 'liquid' state, since the measured values of the internal friction peaks in longitudinal and torsional vibration modes are almost equal. If the SLR were liquid-like under this testing condition (frequency~tens of kHz, strain amplitude~10^{-7}), according to the Stokes' assumptions [19] (it is assumed that there is no hydrostatic relaxation and if the shear modulus G is replaced by the operator $G+\mu\frac{\partial}{\partial t}$, the viscous forces to the total stress will be fully taken into account), the loss Young's modulus E'' and loss shear modulus G'' of a one-dimensional slender bar under vibration can be written as:

$$\begin{cases} E'' = \frac{4}{3}(1+\nu)\mu\omega \\ G'' = \mu\omega \end{cases} \tag{2}$$

Where ν is the Poisson's ratio, μ is a coefficient related to viscoelasticity. Therefore, the ratio of longitudinal internal friction to torsional internal friction should be around 2 / 3. What is more, if the SLR were liquid-like, a breakdown of the shear modulus should be observed as that reported by Qiao [10] and wang [17] using the DMA at the frequency about 0.1 Hz with the strain amplitude about 10^{-4}. However, the relaxation of the shear modulus measured here is only about 10%, indicating that under the conditional of high frequency and micro strain amplitude, the SLR is far from liquid and should be regarded as anelastic solid. To further prove this, we introduce a dimensionless Deborah number (De), as the magnitude of De provides a useful indication whether a material behaves in a more fluid-like or solid-like manner. The Deborah number is defined as De= t_i/t_e, where t_i stands for the internal structural response time under loading and t_e for the macroscopic imposed time of external loading. In the present case, we consider t_e as the characteristic time scale of about 2.5×10^{-5} s (~40KHz). The t_i can be calculated by the Maxwell equation $t_i = \eta/G$,

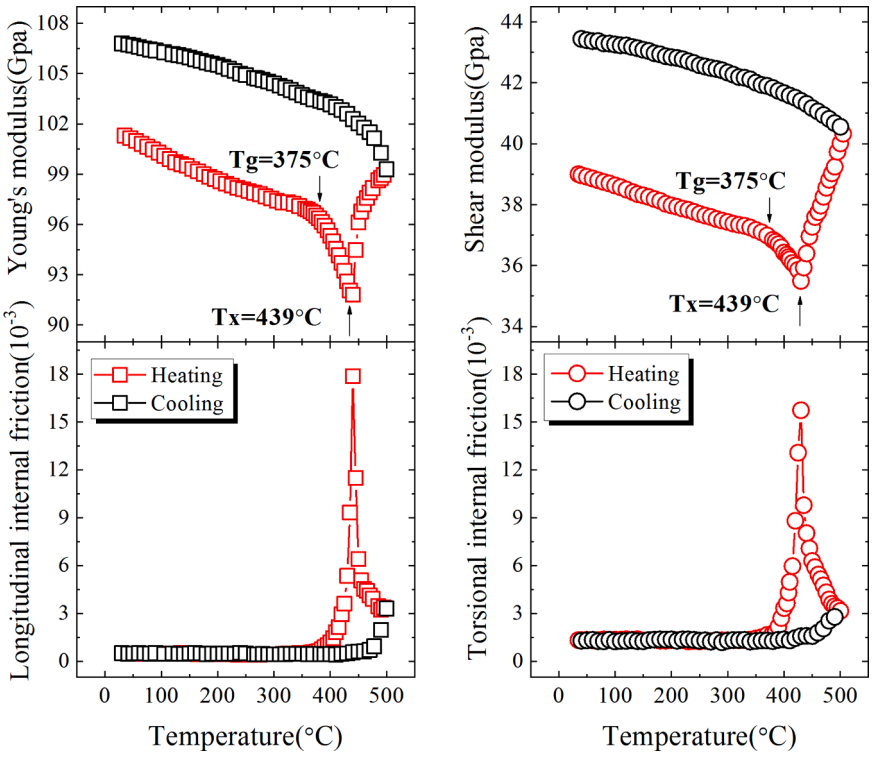

Fig. 3. The temperature dependent elastic moduli and internal frictions of Vit-1 BMG during heating and cooling processes. Left: longitudinal mode; Right: torsional mode.

where η is the dynamic viscosity. By extrapolating the calculated results of Wang [17], we can obtain the dynamic viscosity is about 10^7–10^8kg/m^2·s. The shear modulus we measured here in the SLR is about 35Gpa. So the timescale of t_i is about 3×10^{-4}–$3 \times 10^{-}5$, and the Deborah number is in the range of 12–120. In the case of De>1, metallic glass behaves in a more solid-like manner.

Since the BMG is more solid-like, here we used a standard three-parameter anelastic solid model to better interpret the observed phenomena during glass transition and crystallization. As shown in Fig. 4, the spring (a) with an unrelaxed compliance J_U represents the elastic properties of the BMG outside the SLR. The compliance of spring (b) is considered to be proportional to the volume fraction Y(t) of the supercooled liquid, and its value tends to be (zero) in (outside) the SLR. For convenience, we assumed that the relaxation time τ of the BMG is single, so the viscosity η of the dashpot (c) is $\tau/(\delta J \cdot Y(t))$, representing the viscosity of the BMG in supercooled liquid. When the supercooled liquid fraction Y(t) has the change trend of Fig. 4, we can obtain the change trend of η, which is consistent with Bakke's measurement result [20]. After applying an alternating stress, the elastic compliance J and internal friction Q^{-1} of the BMG can be obtained as follows [21]:

$$\begin{cases} J = J_U + \dfrac{\delta J \cdot Y(t)}{1+\omega^2\tau^2} \\ Q^{-1} = \dfrac{\omega\tau}{1+\dfrac{J_U(1+\omega^2\tau^2)}{\delta J \cdot Y(t)}} \end{cases} \tag{3}$$

Where ω is the measured frequency. It can be seen from Eq. (3) that, when entering the SLR, the BMG soften and Y(t) tends to 1, resulting the decrease of elastic moduli (reciprocal of the elastic compliance J) and rapid increase of internal frictions. When the temperature reaches T_x, the BMG begins to crystallize, Y(t) tends to zero and J_U increase, leading to the increase of the elastic moduli and sharp decrease of internal friction, thus forming the peaks.

Fig. 5(a) shows the temperature dependent Young's modulus and longitudinal internal friction of another Vit-1 specimen measured under two cycles of heating and cooling. It can be seen that, during the first heating process, from room temperature (RT) to 410 °C, the measured results are almost consistent with that in Fig. 3. When the temperature is reduced to 250 °C, it is found that there is an irrecoverable increase in the Young's modulus. This is not caused by the local crystallization, because the XRD pattern of the sample annealed at 410 °C is consistent with that of unheated sample, as shown in Fig. 5(b). This is caused by the annihilation of free volume during the annealing process, resulting in a more compact structure of the BMG [22,23]. When the temperature is raised again to the SLR, δJ decrease (due to the more compact structure after annealing), leading to the weakening of the relaxation strength of Young's modulus (from about 10% to 7%) and the decrease of the longitudinal internal friction peak (from 18×10^{-3} to 8×10^{-3}). When the temperature exceeds 600 °C, the Vit-1 crystallizes completely and shows the characteristics of crystal, i.e., the elastic modulus begins to decrease with the increase of temperature while the internal fiction increase exponentially (high temperature background internal friction). Finally, when the temperature drops to room temperature, it is found that the

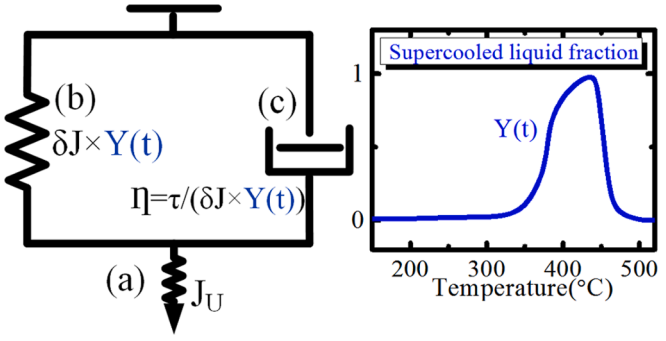

Fig. 4. Three-parameter anelastic solid model for describing the mechanical behavior of the BMG during the glass transition and crystallization.

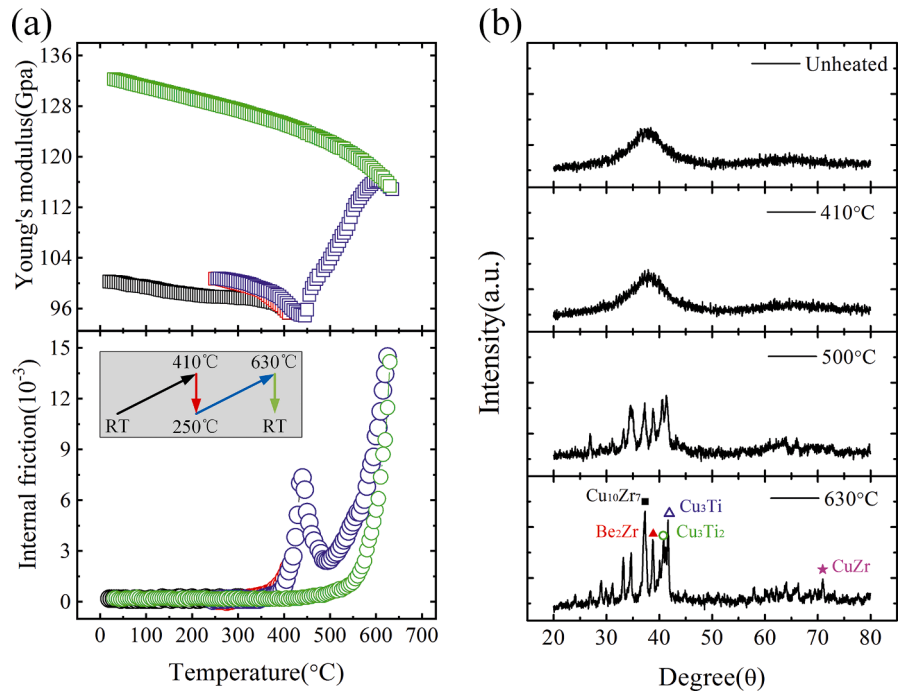

Fig. 5. Mechanical properties and X-ray diffraction patterns (XRD) of Vit-1 BMG. (a) The temperature dependent Young's modulus and internal friction of Vit-1 BMG under cyclic heating-cooling processes; (b) XRD patterns of Vit-1 BMG after different heat treatments: 1) Unheated; 2)Annealed at 410 °C for 30 min; 3) Annealed at 500 °C for 30 min; 4) Annealed at 630 °C for 30 min.

resultant Young's modulus at room temperature (133Gpa) is much larger than that in Fig. 3 (101Gpa), due to that the sample annealed at 630 °C is fully crystallized while the sample annealed at 500 °C is partially crystallized, as shown in the XRD patterns of Fig. 5(b).

Finally, the temperature dependent bulk modulus and Poisson's ratio of vit-1 BMG during the heating process is calculated and drawn together with the exothermic heat flow, as shown in Fig. 6. Apparently, these three curves have something in common: there is an inflection near the glass transition temperature of 375 °C. It is certain that these three quantities are attributed to the unique source, namely the glass transition of BMG. The changes of bulk moduli and Poisson's ratio may be related to the exothermic process before the glass transition.

4. Conclusions

In summary, the temperature dependent Young's modulus, shear modulus and related internal frictions of Vit-1 BMG were measured using M-PUCOT at several tens of kilohertz with the strain amplitude of about 10^{-7}. The measured signals of the M-PUCOT is noiseless and can clearly reflect the changes of the structural transformation of the BMG. The measured internal friction peak values under longitudinal resonance and torsional resonance are almost the same and the moduli relaxations are much weaker than that measured using the low-frequency DMA. This indicates that under the high frequency vibration with the microstrain amplitude, the SLR of BMG should be regarded as anelastic solid instead of viscous fluid under low-frequency vibration with large amplitude. In addition, we found that the internal friction peak value decreases obviously after a preheating process to SLR due to the annihilation of free volume of the BMG and the final values of moduli are proportional to the crystallinity. A three-parameter anelastic model was used to interpret these observed phenomena of BMG. Finally, the bulk modulus and Poisson's ratio of the Vit-1 BMG was presented compared with the exothermic heat flow during the heating process, and it is found that these three curves share the same features.

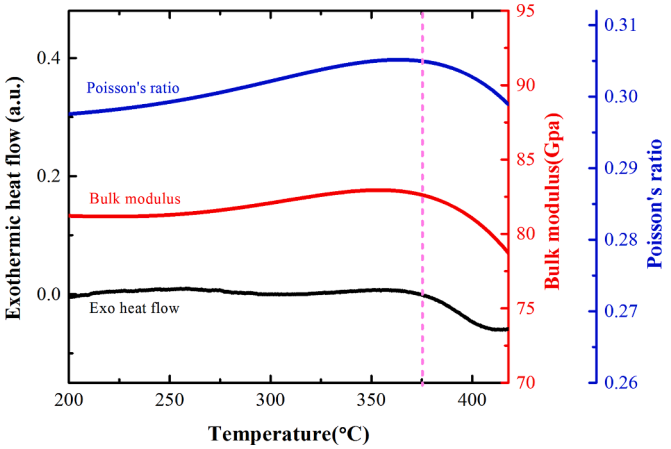

Fig. 6. The temperature dependent exothermic heat flow, bulk moduli and Poisson's ratio of Vit-1 BMG during the heating process.

CRediT authorship contribution statement

Mingyu Xie: Investigation, Data curtion, Writing – original draft. **Gan Ding:** Investigation, Resources. **Minqiang Jiang:** Conceptualization, Writing – review & editing. **Faxin Li:** Conceptualization, Writing – review & editing, Funding acquisition.

Declaration of Competing Interest

The authors declare that they have no known competing financial interests or personal relationships that could have appeared to influence the work reported in this paper.

Acknowledgement

This work is supported by the National Natural Science Foundation

of China under Grant No. 11521202.

Supplementary materials

Supplementary material associated with this article can be found, in the online version, at doi:10.1016/j.jnoncrysol.2021.120754.

References

[1] J.F. Löffler, Bulk metallic glasses, Intermetallics 11 (2003) 529–540.
[2] J. Qiao, J.-.M. Pelletier, Dynamic mechanical relaxation in bulk metallic glasses: a review, J. Mater. Sci. Technol. 30 (2014) 523–545.
[3] M. Chen, A brief overview of bulk metallic glasses, NPG Asia Mater. 3 (2011) 82–90.
[4] R. Busch, E. Bakke, W. Johnson, Viscosity of the supercooled liquid and relaxation at the glass transition of the Zr46. 75Ti8. 25Cu7. 5Ni10Be27. 5 bulk metallic glass forming alloy, Acta. Mater. 46 (1998) 4725–4732.
[5] S.J. Chung, K.T. Hong, M.-.R. Ok, J.-.K. Yoon, G.-.H. Kim, Y.S. Ji, B.S. Seong, K. S. Lee, Analysis of the crystallization of Zr41Ti14Cu12. 5Ni10Be22. 5 bulk metallic glass using electrical resistivity measurement, Scr. Mater. 53 (2005) 223–228.
[6] M. Jiang, M. Naderi, Y. Wang, M. Peterlechner, X. Liu, F. Zeng, F. Jiang, L. Dai, G. Wilde, Thermal expansion accompanying the glass-liquid transition and crystallization, AIP Adv. 5 (2015), 127133.
[7] B. Zhang, F.Q. Zu, K. Zhen, J.P. Shui, P. Wen, Internal friction behaviours in Zr57Al10Ni12. 4Cu15. 6Nb5 bulk metallic glass, J. Phys.: Condensed Matter 14 (2002) 7461.
[8] Y. Hiki, T. Yagi, T. Aida, S. Takeuchi, Low-frequency high-temperature internal friction of bulk metallic glasses, J. Alloys. Compd. 355 (2003) 42–46.
[9] H.-.R. Sinning, Low-frequency internal friction of metallic glasses near Tg A critique of the use of the torsion pendulum, J. Non. Cryst. Solids 110 (1989) 195–202.
[10] J. Qiao, J.-.M. Pelletier, Dynamic universal characteristic of the main (α) relaxation in bulk metallic glasses, J. Alloys Compd. 589 (2014) 263–270.
[11] N. Li, X. Xu, Z. Zheng, L. Liu, Enhanced formability of a Zr-based bulk metallic glass in a supercooled liquid state by vibrational loading, Acta Mater. 65 (2014) 400–411.
[12] T. Ichitsubo, S. Kai, H. Ogi, M. Hirao, K. Tanaka, Elastic and anelastic behavior of Zr55Al10Ni5Cu30 bulk metallic glass around the glass transition temperature under ultrasonic excitation, Scr. Mater. 49 (2003) 267–271.
[13] T. Ichitsubo, E. Matsubara, S. Kai, M. Hirao, Ultrasound-induced crystallization around the glass transition temperature for Pd40Ni40P20 metallic glass, Acta. Mater. 52 (2004) 423–429.
[14] G. Ding, C. Li, A. Zaccone, W. Wang, H. Lei, F. Jiang, Z. Ling, M. Jiang, Ultrafast extreme rejuvenation of metallic glasses by shock compression, Sci. Adv. 5 (2019) eaaw6249.
[15] H. Yizhen, L. Xiao-Guang, A new type of internal friction peak of metallic glasses near Tg, Physica Status Solidi 99 (1987) 115–120.
[16] M. Xie, F. Li, A modified piezoelectric ultrasonic composite oscillator technique for simultaneous measurement of elastic moduli and internal frictions at varied temperature, Rev. Sci. Instrum. 91 (2020), 015110.
[17] Q. Wang, J.-.M. Pelletier, J. Blandin, M. Suery, Mechanical properties over the glass transition of Zr41. 2Ti13. 8Cu12. 5Ni10Be22. 5 bulk metallic glass, J. Non. Cryst. Solids 351 (2005) 2224–2231.
[18] H.-.R. Sinning, F. Haessner, Determination of the glass transition temperature of metallic glasses by low-frequency internal friction measurements, J. Non. Cryst. Solids. 93 (1987) 53–66.
[19] W.J. Ibbetson, An Elementary Treatise On the Mathematical Theory of Perfectly Elastic Solids: With a Short Account of Viscous Fluids, Macmillan, 1887.
[20] E. Bakke, R. Busch, W. Johnson, The viscosity of the Zr46. 75Ti8. 25Cu7. 5Ni10Be27. 5 bulk metallic glass forming alloy in the supercooled liquid, Appl. Phys. Lett. 67 (1995) 3260–3262.
[21] M.S. Blanter, I.S. Golovin, H.-.R. Sinning, Internal Friction in Metallic Materials, 1 ed., Springer, 2007.
[22] Z. Keqin, Study on Structural Free-Volume in Bulk Amorphous Zr_ (41) Ti_ (14) Cu_ (12.5) Ni_ (10) Be_ (22.5) Alloy by Positron Annihilation Techniques, Rare Metal Materials and Engineering 40 (2011) 45–47.
[23] Y. He, R. Schwarz, D. Mandrus, L. Jacobson, Elastic moduli, density, and structural relaxation in bulk amorphous Zr41. 2Ti13. 8Cu12. 5Ni10Be22. 5 alloy, J. Non. Cryst. Solids. 205 (1996) 602–606.